Biochimica et Biophysica Acta, 766 (1984) 245–258
Elsevier

BBA 41538

EPR SPECTRUM AT 4, 9 AND 35 GHz OF HYDROGENASE FROM *CHROMATIUM VINOSUM*

DIRECT EVIDENCE FOR SPIN-SPIN INTERACTION BETWEEN Ni(III) AND THE IRON-SULPHUR CLUSTER

S.P.J. ALBRACHT, J.W. VAN DER ZWAAN and R.D. FONTIJN

Laboratory of Biochemistry, B.C.P. Jansen Institute, University of Amsterdam, P.O. Box 20151, 1000 HD Amsterdam (The Netherlands)

(Received December 27th, 1983)

Key words: Hydrogenase; ESR; (C. vinosum)

EPR spectra at 4, 9 and 35 GHz of hydrogenase isolated from *Chromatium vinosum* have been compared. The spectra at 4 and 35 GHz confirmed our earlier conclusions, made from observations at 9 GHz (Albracht, S.P.J., Kalkman, M.L. and Slater, E.C. (1983) Biochim. Biophys. Acta 724, 309–316), that the irreversibly inactivated enzyme molecules in the preparation give rise to two EPR signals due to the independent non-interacting $S = 1/2$ systems of Ni(III) and a [3Fe-xS] cluster. It was observed that intact enzyme molecules show a complex EPR spectrum caused by a spin-coupled pair of Ni(III) and a $[4Fe\text{-}4S]^{3+}$ cluster. The interaction energy is so weak (approx. 0.01 cm^{-1}) that the 35 GHz spectra of both the Ni(III) and the $[4Fe\text{-}4S]^{3+}$ cluster have the appearance of rather normal $S = 1/2$ spectra with additional splittings as a result of the spin-spin interaction. At lower microwave frequencies, the spectra become increasingly complex but phenomenologically they behave as expected for an exchange-coupled pair of dissimilar ions. The distance between the two spin systems is estimated to be at the most 1.2 nm. The spin-relaxation rate of the Ni(III) ion is dramatically enhanced as a result of the coupling to the rapidly relaxing Fe-S cluster. The g values and so presumably also the ligand fields of Ni in intact and irreversibly inactivated enzyme molecules are identical. This suggests that the specific coordination of the nickel in the enzyme is not the only requirement for activity with artificial electron donors or acceptors, and that the presence of a nearby, intact $[4Fe\text{-}4S]^{3+(3+,2+)}$ cluster might be another essential factor. From the g values and the probable function of Ni in the enzyme we propose, as a working hypothesis, that the nickel ion has five ligands provided by the protein in a square-pyramidal coordination.

Introduction

It has been known for quite some time that hydrogenases contain one or more Fe-S clusters [1–3]. Only recently it was discovered that Ni is essential for the biosynthesis of hydrogenase in *Alcaligenes eutrophus* [4]. Graf and Thauer [5] were the first to report the presence of Ni (0.8 atom per mole of enzyme) in a purified hydrogenase (from *Methanobacterium thermoautotrophicum* strain Marburg). The nickel, which was qualitatively and quantitatively characterized by EPR as Ni(III), can be reduced to Ni(II) by H_2 [6]. Ni was later detected in hydrogenases isolated from *A. eutrophus* [7], *M. thermoautotrophicum* strain ΔH [8,9], *Desulfovibrio gigas* [10–13], *Desulfovibrio desulfuricans* [14,15], *Chromatium vinosum* [16] and *Vibrio succinogenes* [17]. In many cases a characteristic [6,18] EPR signal of Ni(III) was also detected [9–15]. All these enzymes are so-called 'uptake' hydrogenases, the physiological role of which is presumably to take up hydrogen from the environ-

ment to supply the cell with reducing equivalents for growth. No EPR signal due to nickel has thus far been reported for the other class of hydrogenases, the 'production' type of enzymes.

The enzyme from *C. vinosum*, as first purified in 1975 by Gitlitz and Krasna [19], displayed only one prominent EPR signal in the oxidised state. This signal, here called signal 1, was attributed to a $[4Fe\text{-}4S]^{3+}$ cluster [20] and it was believed [20] that the enzyme itself showed no other signal in either the oxidised or reduced state. A different purification procedure has been developed in our laboratory [21] and in our hands the enzyme shows an additional prominent signal, signal 2, which selectively disappears during contact with 2-mercaptoethanol or after removal of oxygen. We have shown [16] that under certain conditions signal 1 can be induced simultaneously with a $g = 4.3$ signal from Fe(III) and we concluded that signal 1 arises from a [3Fe-*x*S] cluster, and that the intact enzyme molecules thus contain a [4Fe-4S] cluster which can give rise to signal 2. This conclusion was strengthened by the effect of ^{57}Fe ($I = 1/2$) [16]. Since signal 2 is not due to a simple $S = 1/2$ species [21], we proposed that the $[4Fe\text{-}4S]^{3+}$ cluster has an interaction with another paramagnetic redox center in the enzyme. Evidence for the presence of this second centre was borne out by the finding [21] that the reduced enzyme, in the absence of H_2, can reduce two equivalents of ferricytochrome *c*.

Recently, we characterised a third EPR signal composed of an overlap of two $S = 1/2$ spectra, both due to Ni(III) [22]. In all our preparations, the total intensity of this signal 3 is equal to that of the signal of the [3Fe-*x*S] cluster. From the lack of correlation between the activity of the enzyme and the intensity of the signal of the 3-Fe cluster [16], we concluded that signal 1, and consequently also signal 3, arise from irreversibly inactivated hydrogenase molecules.

The situation with the hydrogenase activity of *C. vinosum* is complicated by the finding that during the purification procedure, the activity often behaves as two apparently independent enzymes [22] with different EPR characteristics. The type-I preparation, which usually forms the major fraction, shows all the signals to be discussed in this report. The type-II preparation, however, lacks signal 2 and displays only one signal due to Ni(III). At temperatures below 30 K, a complicated set of lines in the $g = 2.1\text{–}2.4$ region, here called signal 4, was detected in the type-I preparation but not in type II [22]. These findings are summarised in Table I and Fig. 1.

We have previously shown [22] that signal 2 disappears within 12 min during contact of the type-I preparation with excess ascorbate plus 5 μM phenazine methosulphate. At the same time, both signal 1 and signal 3 increase, the spin concentrations of the corresponding species remaining equal to one another. We interpreted this finding as due to the reaction: Ni^{3+}----$[4Fe\text{-}4S]^{3+}$ (spin-coupled) $\rightarrow Ni^{3+} + [3Fe\text{-}x S]$ (uncoupled). Incidentally, we noticed that also signal 4, the origin of which was not understood, disappeared during this treatment [22].

Preliminary redox titration of the enzyme (J.W. Van der Zwaan, unpublished observations) indicated that signal 4 also originates from intact enzyme molecules. In this study we show, by comparison of EPR spectra at 4, 9 and 35 GHz, that signal 4 is due to Ni(III) interacting with the $S = 1/2$ system of the $[4Fe\text{-}4S]^{3+}$ cluster. Likewise, it is concluded from the spectra of Signal 2 at these microwave frequencies that it arises from a $[4Fe\text{-}4S]^{3+}$ cluster interacting with the $S = 1/2$ system of Ni(III).

Materials and Methods

C. vinosum, strain DSM 185, was grown in a 700-1 batch culture [22]. The enzyme was purified exactly as described previously [21] and dissolved in 50 mM Tris-HCl buffer (pH 7.4). S-band (4 GHz) spectra were obtained with a Bruker ER 061 SR microwave bridge plus a Bruker ER 6102 SR re-entrant cavity in combination with a Varian E-9 EPR spectrometer. A field-modulation frequency of 10 kHz was employed. X-band (9 GHz) spectra were obtained with a standard Varian E-9 EPR spectrometer, while for spectra at Q-band (35 GHz) this spectrometer was used in combination with the Varian E-110 microwave bridge plus the E-266 cavity; in both cases, the field-modulation frequency was 100 kHz. Cooling of the sample at X- and S-band was performed by using the helium-flow system as described by Lundin and

Aasa [23] with suitable changes for the dimensions of the cryostat at S-band. Cooling at Q-band was as described in Ref. 24. The magnetic field was calibrated with an AEG Magnetic Field Meter. The X-band frequency was measured with a HP 5246L electronic counter, supplemented with a HP 5255A frequency converter. The frequencies at S- and Q-band were derived from the field value of the absorption of α,α'-diphenyl-β-picrylhydrazyl (DPPH). The E-9 spectrometer console, used with all three microwave frequencies, was connected to a HP 2100 minicomputer via a data acquisition front-end septum based on a PDP 11-03 microprocessor and spectra were stored on magnetic disc for later retrieval. Other experimental details were as described in Refs. 25 and 26.

Results

The present study was initiated as the result of a preliminary redox titration of the enzyme. It was found (J.W. Van der Zwaan, unpublished observations) that on lowering the potential from −19 mV to −38 mV, all the lines belonging to signal 4 disappeared simultaneously with those of signal 2. Since it had previously been concluded that signal 2 is a property of active enzyme molecules [22], this finding suggested that also signal 4 belongs to such molecules. The complex line shapes of both signal 4 and signal 2 were not understood. We, therefore, have examined the enzyme by EPR at two microwave frequencies different from X-band (9 GHz), namely at S-band (4 GHz) and at Q-band (35 GHz). It should be noted that all experiments described in this section were carried out with the type-I preparation [22].

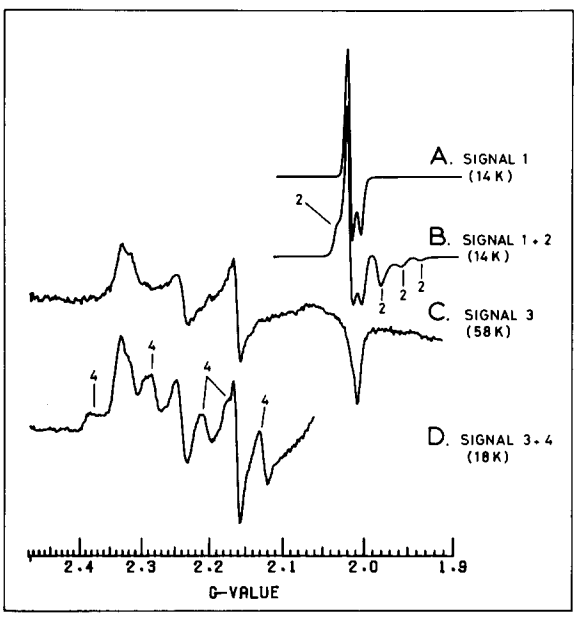

Fig. 1. Inventory of the four EPR signals observable in hydrogenase from *C. vinosum*. A, signal 1; B, signal 1 + signal 2; C, signal 3; D, signal 3 + signal 4. The signals 1, 2 and 4 are not detectable at high temperatures. Signal 2 disappears after anaerobiosis or addition of 2-mercaptoethanol. Strong *g*-anisotropy causes the signals 3 and 4 to be much smaller in amplitude than the signals 1 and 2, although they are of comparable intensity.

TABLE I

INVENTORY OF EPR SIGNALS AT 9 GHz IN SOLUBLE HYDROGENASE FROM *C. VINOSUM*, THUS FAR DETECTED IN OUR LABORATORY

Signal	Presumed origin	Enzyme preparation	
		Type I [a]	Type II [a]
1 [b]	[3Fe-*x*S]	+	+
2 [c]	Ni^{3+}---$[4Fe\text{-}4S]^{3+}$	+	−
3 [b]	Ni-a, Ni-b	+	+ [d]
4	unknown	+	−

[a] For properties see Ref. 22.

[b] Signals originate from irreversibly inactivated enzyme molecules.

[c] Signal is considered to be due to an interaction of Ni(III) and a $[4Fe\text{-}4S]^{3+}$ cluster in intact enzyme molecules [22]. It slowly disappears after addition of 2-merceptoethanol or after anaerobiosis.

[d] Only one signal can be detected, similar in shape to the signal of Ni-a of the type-I preparation.

Signal 1 and signal 2

Although we have previously published a Q-band spectrum of hydrogenase [21], no detailed information could be abstracted from the trace at that time due to the poor signal-to-noise ratio. The effective sensitivity of Q-band EPR is much lower than that at X-band, mainly because of the limitations in the size of the sample. We have now inspected a more concentrated sample of the type-I preparation that also enabled detection of the Ni signals in Q-band. In Fig. 2 the EPR spectra in the $g = 2$ region at X- and Q-band are represented on a g scale. Signal 1 is responsible for the main line

at $g = 2.02$ at both frequencies. All other lines in the Q-band spectrum belong to signal 2. The meaning of the bars will be clarified in the discussion. Reaction of the enzyme with 2 mM 2-mercaptoethanol for 2.5 h at 0°C, carried out in a separate Q-band EPR tube, reduced the amplitudes of the lines of signal 2 by 65%, without affecting the intensity of signal 1. In this way, the individual line shapes of signal 1 and signal 2 could be obtained via subtraction; they are displayed in Fig. 3. The same Q-band EPR tube was used for both the X- and the Q-band measurements. The shape of signal 1 (traces C and D, Fig. 3) and the position of its lines on a g scale are the same at the two microwave frequencies, as is to be expected for an independent $S = 1/2$ system. The line widths in the X-band spectrum, expressed in units of g, are significantly greater than those in the Q-band spectrum, indicating that unresolved splittings, as caused by weak interactions with magnetic nuclei or electron spins, and not g strain

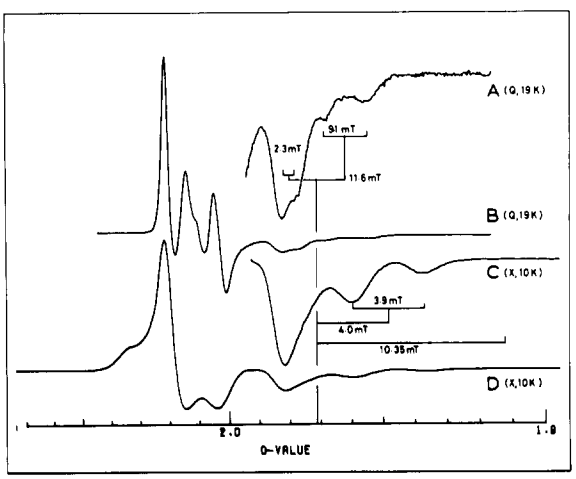

Fig. 2. EPR spectra at Q- and X-band of the enzyme as isolated. Protein concentration, 10.5 mg/ml; specific hydrogen production activity of the enzyme, 13 μmol/min per mg. The same Q-band EPR tube was used for both measurements. EPR conditions for Q-band (traces A and B); microwave frequency, 35243 MHz; temperature, 19 K; microwave power, 0.5 mW; modulation amplitude, 0.63 mT. Trace A is an average of nine scans, trace B an average of four scans. Conditions for X-band (traces C and D): microwave frequency, 9269.9 MHz; temperature, 10 K; microwave power, 2.2 mW; modulation amplitude, 0.63 mT. The traces A and C are enlarged representations of the high-field parts of the spectra B and D, respectively. All spectra are converted to the same g scale.

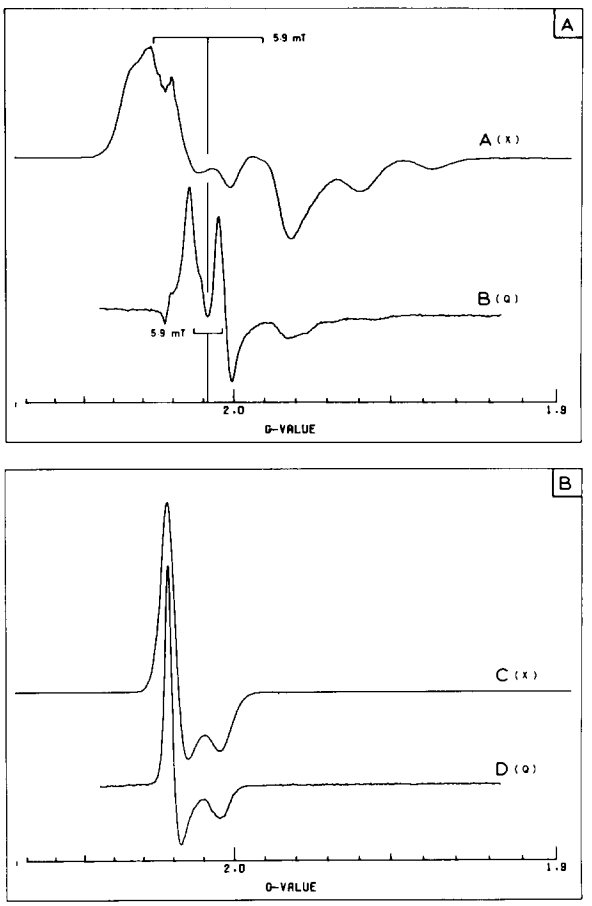

Fig. 3. The line shapes of signal 2 and signal 1 at X- and Q-band. The enzyme was mixed with 2 mM 2-mercaptoethanol in a separate Q-band tube. After 2.5 h at 0°C, the sample was frozen in liquid nitrogen. Spectra were recorded at X- and Q-band. In the case of the Q-band measurements, care was taken to tune the experimental microwave frequency as closely as possible to the frequency used in Fig. 2. The spectra were then subtracted from the related spectra in Fig. 2, using the criterion that signal 1 must disappear from the difference (traces A and B). The difference spectra were then subtracted from the corresponding spectra obtained after the reaction with 2-mercaptoethanol to give the spectrum of signal 1 (traces C and D). The EPR conditions were as in Fig. 2.

[27–29] contribute most to the width at X-band. The spectra obtained for signal 2 (traces A and B, Fig. 3) at the two microwave frequencies differ considerably in shape and in the positions of the lines. It can be seen that the region of the spectra between $g = 2.02$ and 2.03 suffers from slight artifacts of the subtraction procedure. Since we store 1000 datum points from each individual

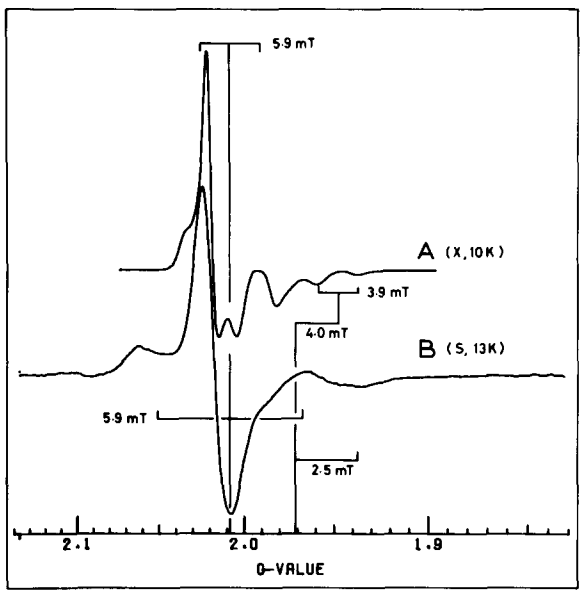

Fig. 4. EPR spectra of the enzyme at X- and S-band. An X-band tube was used for both measurements. EPR conditions for X-band (trace A): as in Fig. 2. Conditions for S-band (trace B): microwave frequency, 3953 MHz; temperature, 13 K; microwave power, 2 mW; modulation amplitude, 0.4 mT.

spectrum, it is unavoidable that a small mismatch occurs during the alignment of the spectra which were otherwise recorded at nearly, but not precisely the same, experimental frequency. Especially when sharp signals like those in Fig. 3, traces C and D, are to be removed via subtraction of spectra, this mismatch is clearly noticeable (see Fig. 3, traces A and B). It is only now, with these detailed spectra, that we can observe that also the less intense high-field lines (cf. Fig. 2) have different positions on a g scale at X- and Q-band, proving that none of these peaks represent real g values.

The enzyme, filled in an X-band tube, has also been studied at S-band. A comparison of the $g = 2$ region in X- and S-band is shown in Fig. 4. The resolution between the $g_\perp$ and the $g_\parallel$ lines of signal 1, still observable in X-band, is lost at S-band due to further broadening by unresolved splittings. The shape of signal 2 has completely changed. Whereas at X-band one can detect four distinct absorption lines at $g = 2.035$, 1.98, 1.96 and 1.935, there are only two broad lines at $g =$ 2.06 and $g = 1.935$ and a shoulder at $g = 1.985$ detectable at S-band. The line at $g = 2.10$ is not due to signal 2 but to signal 4 (see later).

Signal 3 and signal 4

In Fig. 5, EPR spectra in the $g = 2$–2.4 region, recorded at three different microwave frequencies, are displayed. The X- and Q-band spectra have been recorded at a relatively high temperature, where the signals 1 and 2 are absent due to relaxation broadening. The S-band spectrum was obtained at 13 K. We have previously shown [22] that the X-band spectrum of Fig. 5, which we call signal 3, is readily simulated as a superposition of two $S = 1/2$ spectra both with a rhombic g-tensor. The shape of the Q-band spectrum is fully in line with this interpretation, since all lines appear at the same g values as in X-band. Also the S-band spectrum shows these same lines (the line around $g = 2.1$ is due to signal 4; see below). When expressed in units of g, the widths of the lines increase from Q-band to S-band, indicating an important contribution of unresolved hyperfine and/or other interactions. The measured peak-to-peak widths in field units of the $g = 2.16$ lines were 1.45 mT, 1.7 mT and 3.2 mT at S, X and Q-band, respectively. According to our previous experience with the enzyme [16,22], signal 3 is due to two forms of Ni(III), Ni-a and Ni-b, both present in irreversibly inactivated enzyme molecules.

At low temperatures, various additional lines clearly appeared (Fig. 6). Spectra at two different microwave powers are displayed to emphasise the fact that the new lines do not saturate easily, in contrast to the lines of signal 3. The extra lines have in the Q-band spectrum a line shape interpretable at first sight on the basis of normal $S = 1/2$ line shapes plus a hyperfine interaction with a magnetic moment of 1/2. The g_y line of Ni-a at $g = 2.16$ has, at Q-band, two satellite lines symmetrical around the central line. The satellite lines are due to signal 4 and are far less easily saturated than the central line, which is due to signal 3. This can also be observed, although less clearly for the g_y line of Ni-b at $g = 2.24$. Assuming that the linewidth of the three lines around $g = 2.16$ is the same, the splitting is calculated to be 12 mT; for the $g = 2.24$ line the splitting is estimated to be about 10 mT. As a first approximation, it might be concluded from the Q-band spectrum that at low temperatures, an extra signal, signal 4, appears which has the same g values as observed for signal 3 (Fig. 5), but where a hyperfine splitting due to a

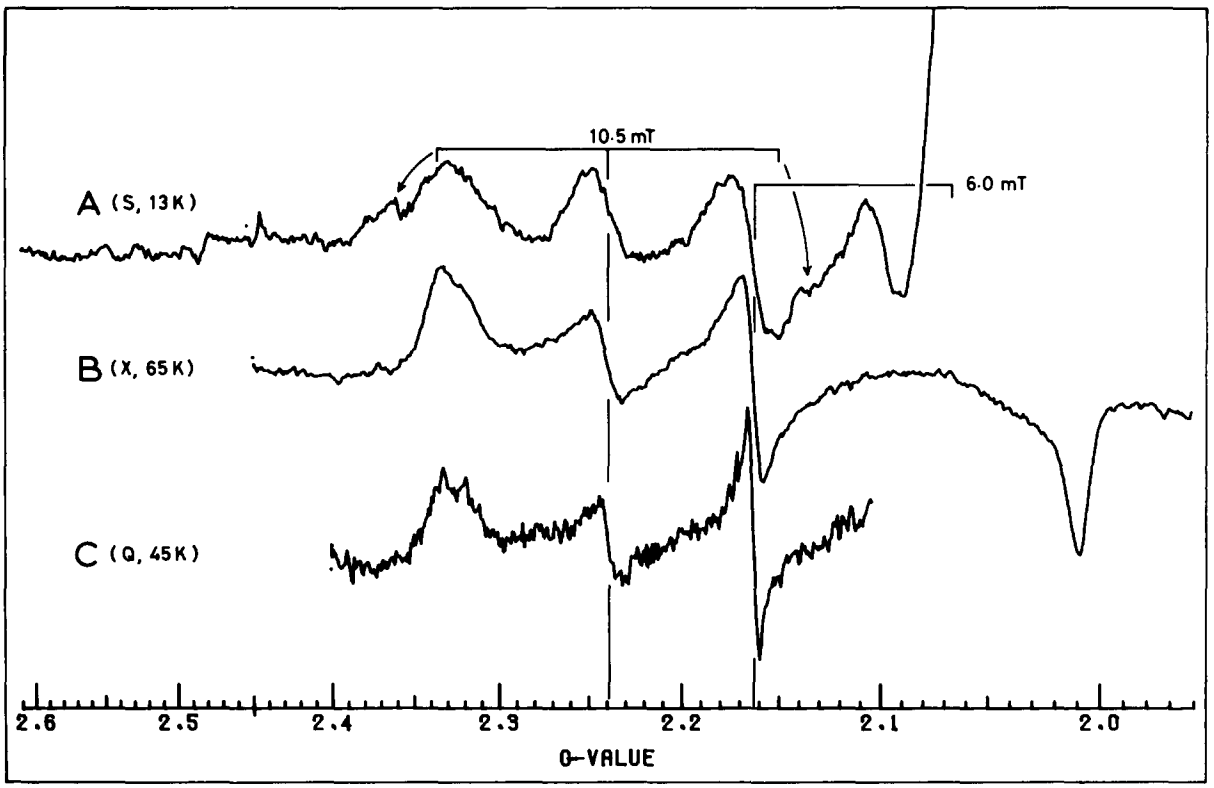

Fig. 5. EPR spectra of hydrogenase in the $g = 2.1–2.4$ region at S-, X- and Q-band. For X- and Q-band measurements (traces B and C, respectively), the same Q-band EPR tube as used for Fig. 2 was employed. For S-band (trace A), the X-band tube of Fig. 4 was used. EPR conditions for S-, X- and Q-band: microwave frequencies, 3953, 9269.5 and 34460 MHz; temperatures, 13, 65 and 45 K; microwave powers, 2, 2 and 0.5 mW; modulation amplitudes, 0.9, 1.0 and 1.25 mT. Spectra were averages of six (S-band), nine (X-band) and nine (Q-band) scans.

magnetic moment of 1/2 causes a different line shape. Inspection of the X-band spectrum of signal 4 around $g = 2.16$ also reveals two satellite lines (marked with an arrow) with a similar line width as the $g = 2.16$ line of signal 3, but their centre now has a different g value. Also the peak-to-peak distance of these lines is only about 8.5 mT, whereas this distance is 15.5 mT in Q-band. The peak-to-peak distance of the satellite lines around the $g = 2.24$ line in the X-band spectrum is about 12 mT. The line around $g = 2.38$ observed in the X-band spectrum is apparently new, but since it is presumably due to a splitting, it might be hidden under the main peak around $g = 2.33$ in the Q-band spectrum. At S-band, the lines of signal 4 probably spread out to an extent that makes them difficult to detect (Fig. 5, trace A); the line at $g = 2.10$ is thought to be the only obvious representative of signal 4 at this microwave frequency. All lines of signal 4 decrease to about 35% of their original amplitude by the treatment with 2-mercaptoethanol. The magnitude of this effect is thus equal to that of the effect on signal 2 as measured in the same EPR tube. The best approximation of the separate line shape of signal 4 at X-band, obtained via a difference of the spectra before and after the treatment with 2-mercaptoethanol, is represented in Fig. 7 and is not readily interpretable. The signal-to-noise ratio of the normal Q-band spectra of the samples was too low for a good difference spectrum. However, an indication of the changes in the Q-band spectrum caused by 2-mercaptoethanol could be obtained from spectra recorded under rapid-adiabatic-passage conditions [30]. Fig. 8 shows these spectra, which are now absolute spectra and not

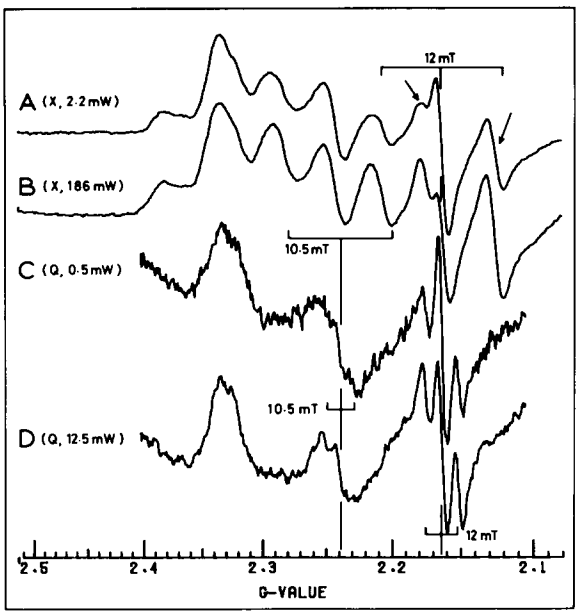

Fig. 6. Low-temperature spectra in the $g = 2.1-2.4$ region at X- and Q-band. The same tube as in Fig. 2 was used for Q-band (traces C and D), whereas the X-band tube of Fig. 4 was employed for X-band (traces A and B). EPR conditions for X-band: microwave frequency, 9268.2 MHz; temperature, 16 K; microwave power, 2.2 mW for A and 186 mW for B; modulation amplitude, 0.32 mT for A and 0.63 mT for B. The gain for A was 6.25-times greater than for B. Conditions for Q-band: microwave frequency, 34472 MHz; temperature, 24 K; microwave power, 0.5 mW for C and 12.5 mW for D; modulation amplitude, 1.25 mT. Both Q-band spectra were averages of nine scans. The gain for C was 2.5-times greater than for D.

first derivatives, before and after the treatment, together with a difference spectrum. The latter demonstrates the disappearance of the satellite lines around $g = 2.24$ and 2.16, showing that these lines, together with the changes around $g = 2.335$, must correspond to the complicated set of lines observed at X-band (Fig. 7, trace C). From the Q-band difference spectrum (Fig. 8, trace C), the distance of the two pairs of lines around the g_y lines at $g = 2.24$ (Ni-b) and $g = 2.16$ (Ni-a) are measured to be 10.5 and 12 mT, respectively.

Temperature dependence of the signals 2 and 4 at X-band

Fig. 9 displays X-band spectra of the enzyme at different temperatures. It can be seen that the signals 1, 2 and 4 gradually disappear above 20 K

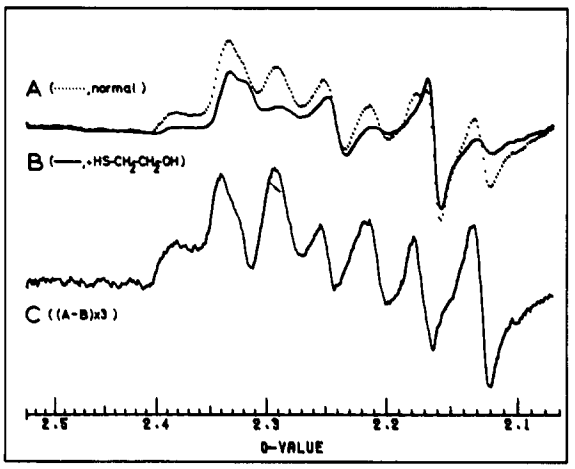

Fig. 7. Effect of treatment with 2-mercaptoethanol on the $g = 2.1-2.4$ region of the spectrum. The tubes used for Figs. 2 and 3 were also employed here. A (·····), spectrum before the treatment; B (———), spectrum after the treatment; C, 3× enlarged difference spectrum A minus B, using the criterium that the line at $g = 2.16$ must disappear from the difference. EPR conditions: microwave frequency, 9269.2 MHz; temperature, 15 K; microwave power, 8.5 mW; modulation amplitude, 1.0 mT. Spectra A and B were averages of nine scans.

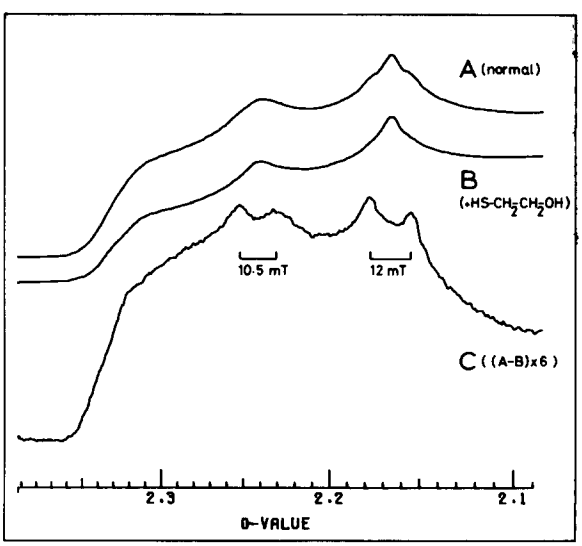

Fig. 8. Q-band spectra of the enzyme before and after treatment with 2-mercaptoethanol recorded under rapid-passage conditions. The same tubes as used for Figs. 2 and 3 were used. A, before the treatment; B, after the treatment; C, 6× enlarged difference spectrum. EPR conditions; microwave frequency, 35242 MHz; temperature, 13 K; microwave power, 32 mW; modulation amplitude, 0.8 mT. The passage signals were obtained using the dispersion mode of the bridge.

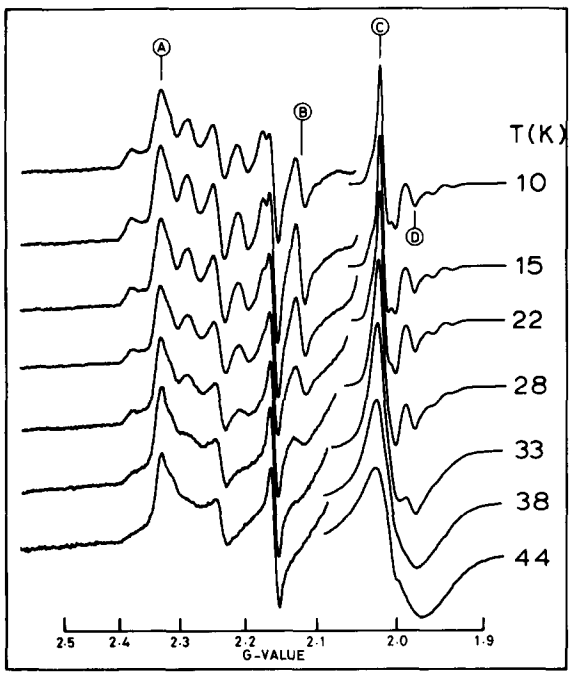

Fig. 9. EPR spectra of hydrogenase at different temperatures. EPR conditions: microwave frequency, 9268 MHz; temperatures as indicated at each trace; microwave power, 2.2 mW; modulation amplitude, 1.25 mT. The relative gains for the left- and the right-hand parts of the spectra were, respectively: 62.5 and 1 (10 and 15 K), 62.5 and 1.6 (22 K), 62.5 and 3.1 (28 K), 78 and 7.8 (33 K), 100 and 15.6 (38 K) and 100 and 31.3 (44 K).

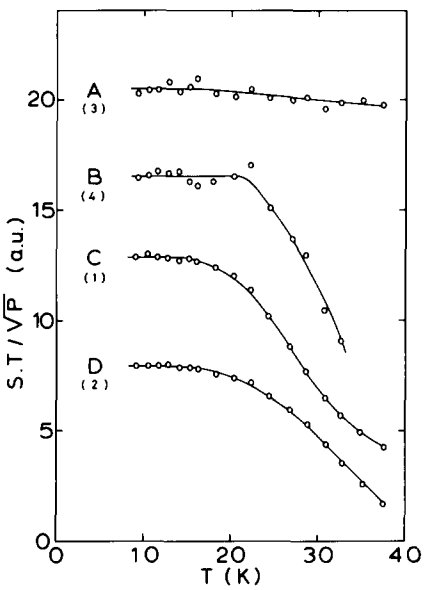

Fig. 10. Temperature dependence of the signals 1–4 measured under non-saturating conditions. The amplitudes of a characteristic line of each of the four signals, marked as A–D in Fig. 9, were measured at temperatures between 8 and 37.5 K. A, signal 3; B, signal 4; C, signal 1; D, signal 2. Two calibrated carbon resistors were present in the sample on both sides of the measuring area of the cavity at a mutual distance of 2.5 cm. The temperature gradient over the sample was 1.5 K (at 8 K) to 3 K (at 37.5 K). The average of the temperatures measured with the resistors was taken as the sample temperature. The microwave power was always non-saturating for any signal and varied between 0.018 mW (at 8 K) and 0.9 mW (at 37.5 K). S, signal amplitude; T, temperature; P, microwave power; a.u., arbitrary units.

and that only signal 3 survives the rise in temperature. A graphic representation of the temperature profile of a characteristic line of each of the four signals marked A–D in Fig. 9, is given in Fig. 10. In this case, the temperature of the sample was directly measured during the recording of the spectra with two calibrated carbon resistors in the frozen sample, one just above and the other just below the measuring area of the cavity, taking the average temperature, calculated from the measured resistances [31], as the sample temperature. Disregarding the effect of relaxation broadening for the moment, the amplitude of a non-saturating $S = 1/2$ signal, normalised for temperature, microwave power and instrumental gain, should be independent of temperature. When two $S = 1/2$ systems are interacting by way of electrostatic exchange, such an interaction might be detected via an abnormal temperature dependence of the signal around a temperature where J, the exchange interaction, is equal to kT [32,33]. Trace A in Fig. 10 represents the behaviour (in X-band) of the g_x line of the Ni(III) signal of irreversibly inactivated molecules. As expected, the signal is proportional to the reciprocal temperature and the slight deviation is ascribed to overlapping features of signal 4 that disappear at higher temperatures (see Fig. 9). The temperature dependence of the high-field line in signal 4 (at $g = 2.13$) is represented by trace B. A rather abrupt decrease of the line amplitude is noticed above 20 K. At 40 K, this line has completely disappeared. Signal 1 (trace C) starts disappearing already above 13 K. The $g = 1.98$ line of signal 2 also decreases in amplitude above 13 K (Fig. 10, trace D). The decrease is probably more

pronounced than indicated in trace D, since the overlapping, quickly broadening signal 1 counteracts this decrease. Since all traces in Fig. 10 are flat below 13 K, we expect any exchange interaction to be smaller than 1 cm^{-1}. We have never observed any half-field signal under any condition.

Discussion

Signals with true g values

Among the great many absorption lines in the low-temperature EPR spectrum of the type-I hydrogenase preparation of *C. vinosum* as we isolate it, there are two signals which have properties as expected for an independent $S = 1/2$ system. The lines of signal 1 clearly behave as true g values (Figs. 3 and 4). We, therefore, interpret its temperature dependence at X-band (Fig. 10, trace C) in terms of a normal Curie dependence at low temperatures and an amplitude decrease above 13 K due to relaxation broadening. On basis of other properties this signal can be attributed [16,22] to a [3Fe-xS] cluster [34] in the oxidised state.

Also the lines of signal 3 (Fig. 5) behave as expected for independent $S = 1/2$ systems and since the spin relaxation is rather slow in this case, the line amplitudes are nicely proportional to the reciprocal temperature over a wider temperature region (Fig. 10, trace A). As argued earlier [22], the complete signal is a superposition of two $S = 1/2$ signals with rhombic g-tensors and both arise from Ni(III). The total intensity of signal 3, which is a measure for the concentration of Ni-a plus Ni-b, is always equal to the intensity of signal 1, which reflects the concentration of the [3Fe-xS] cluster. We have shown earlier [16,22] that these paramagnets reside in irreversibly inactivated enzyme molecules. Thus, part of our preparation consists of inactive molecules having one Ni-a plus a [3Fe-xS] cluster and others having one Ni-b and a [3Fe-xS] cluster. The ratio of these different molecules is preparation-dependent and we do not know which factors control this ratio. Whether or not the [3Fe-xS] clusters in the two types of inactive molecule are different cannot be abstracted from their EPR spectra, since signal 1 apparently consists of only one signal. The amount of irreversibly inactivated enzyme molecules and hence the absolute intensity of signal 1 and signal 3 is preparation-dependent as well and varies between 10 and 50% of the total enzyme concentration [16].

Signals with frequency-dependent g values

Both signal 2 (Figs. 2–4) and signal 4 (Figs. 6–8) show lines the position of which on a g-scale is dependent on the microwave frequency. From our earlier studies on the enzyme [16], we know that the activity is only associated with those hydrogenase molecules in which the Fe-S cluster has not been degraded to a [3Fe-xS] type of cluster and we have provided evidence that the intact enzyme molecules contain a $[4Fe\text{-}4S]^{3+(3+,2+)}$ cluster. Such a cluster, in the oxidised state, is expected to give rise to an EPR signal around $g = 2$ at temperatures below 30 K (at X-band). Since signal 2 has such properties and since ^{57}Fe ($I = 1/2$) but not ^{61}Ni ($I = 3/2$) broadens all lines of this signal [16], a close correlation between signal 2 and the $[4Fe\text{-}4S]^{3+}$ cluster was proposed. The present study provides clear evidence for the suggestion, raised already in our first study [21], that a spin-spin interaction probably complicates the appearance of the spectrum. As obvious from the results described here, Ni(III) presents itself as the partner ion. Inspection of the Q-band spectra in Fig. 6 shows that signal 4, i.e., the lines that only show up at low temperatures (compare with Fig. 5; see also Fig. 9), has in fact the same shape and g values as observed with signal 3, but its lines are split up in pairs. Since signal 3 is due to Ni(III), this strongly suggests that also signal 4 arises from Ni(III).

The general EPR properties of a pair of spin-coupled, dissimilar ions have been summarised by Abragam and Bleany [32]. A weak exchange interaction causes a doublet structure in the EPR spectra around the g values of the individual ions. The distance of the lines is equal to the component of the overall exchange interaction in the corresponding direction. In 1972, a spin-spin interaction was first recognised in a biological molecule, namely an interaction between Mo(V) and an Fe-S cluster in xanthine oxidase [35]. Later, such interactions were observed in a variety of biological systems, e.g., an interaction between two $[4Fe\text{-}4S]^{1+}$ clusters in some bacterial ferredoxins [36], an interacting radical pair of ubisemiquinones in succinate : ubiquinone oxidoreductase of the

mitochondrial respiratory chain [37], an interacting pair of Co(II) and an organic free radical observed during catalysis by enzymes utilising coenzyme B-12 [38] and interacting Fe-S clusters in chloroplasts [39]. The general theory of spin-spin interaction has been worked out in detail by Coffman and Buettner [40–41]. They had earlier used their analysis better to understand the spectra of the Co(II)-radical pair in coenzyme B-12-dependent enzymes [42] and also reinterpreted the spectra of the Mo(V)/Fe-S cluster pair in xanthine oxidase [41] as earlier published by Lowe et al. [35,43].

We now turn our attention again to the EPR spectra of hydrogenase. Since contact of the enzyme with 2-mercaptoethanol decreases the amplitudes of the lines of signal 4 and signal 2 to the same extent, without affecting the intensities of the signals 1 and 3, we conclude that signal 2 and signal 4 are both due to the spin-coupled pair. Although we suspect that a specific reduction of the pair by the thiol takes place, this remains to be established. The Q-band spectrum of signal 4 (Fig. 6, trace D) shows that its g values are the same as those for signal 3. In addition, it can be concluded that the specific ratio of Ni-a and Ni-b present in signal 3, displayed by irreversibly inactivated molecules, is reflected also in signal 4, which is considered to arise from intact molecules. At Q-band, the energy of the Zeeman interaction appears to be large, compared to the interaction energy. The spectrum of signal 4, in particular the features around the g_y values at $g = 2.24$ and 2.16, can be readily approximated by a simulation on the basis of the two $S = 1/2$ systems of Ni-a and Ni-b [22] plus an additional hyperfine splitting (not shown). The intensity ratios required for the simulation of the signals from Ni-a and Ni-b in signal 3 (Fig. 5, trace C) and in signal 4 (as in Fig. 6, trace D) were the same (1 : 0.55). The magnitude of the splittings around the g_y type of lines is best estimated from the Q-band spectra in Fig. 8. From trace C, the splittings at $g = 2.24$ (Ni-b) and $g = 2.16$ (Ni-a) are measured as 10.5 and 12.0 mT, respectively. A pair of lines around $g = 2.24$ with a distance of 10.5 mT can also be observed in the X-band spectrum (see the bars in Fig. 6 under the traces A and B) and less clearly in the S-band spectrum (see the bars in Fig. 5); here only the top of the low-field line and the trough of the high-field line, indicated by the arrows, can be observed. The simplest explanation is to assume that the splitting is due to an exchange interaction of about 0.011 cm^{-1}. The pair around $g = 2.16$ has a slightly different behaviour. At Q-band, the pair is nicely centered around $g = 2.16$ with a splitting of 12.0 mT (Fig. 6, trace D), but at X-band, the splitting is clearly less and the centre of the lines has shifted to a lower g value (compare the peaks marked with the arrows in Fig. 6, trace A with the indicated 12 mT spacing of the bar). The distance from $g = 2.16$ to the high-field line is now 5.2 mT; at S-band (Fig. 5) this distance has further decreased to 4.2 mT (compare with the indicated 6 mT spacing of the bar). This apparently irregular behaviour is not understood. A splitting is also resolved in the g_x region at $g = 2.33$ on going from Q- to X-band (Fig. 6). From these observations, we conclude that our preparation contains two kinds of intact hydrogenase molecule: one with a Ni-a ion in interaction with a [4Fe-4S] cluster and the other with a Ni-b ion interacting with such a cluster. The rate of conversion of the [4Fe-4S] cluster to a [3Fe-xS] cluster during the purification of the enzyme is apparently the same for both types of molecule. We do not understand the causes responsible for the varying ratio of Ni-a/Ni-b in the enzyme preparation.

The conclusion above implies that, in principle, we might expect to detect also two kinds of signal from two different $[4Fe\text{-}4S]^{3+}$ clusters with an intensity ratio similar to that of the signals of Ni-a and Ni-b in signal 4. This possibility can, however, be eliminated by the finding that the X-band line shape of signal 2, in enzyme preparations in which we found nearly exclusively Ni-b, was identical to that found in other preparations (not shown).

With this knowledge, the Q-band spectrum of signal 2 in Figs. 2 and 3 is interpreted to have an axial g-tensor with $g_{\parallel} = 1.9712$ and $g_{\perp} = 2.0086$ (see vertical bars in Fig. 2 and in Fig. 3, traces A and B). such a g-value set is most unusual for a normal $[4Fe\text{-}4S]^{3+}$ cluster. The $g_{\perp}$ line is split into two lines with a distance of 5.9 mT (Fig. 3, trace B). A similar pair of lines, centred at the same g value, is also observed at X-band (Fig. 3, trace A), where they form the main lines of the spectrum. At S-band (Fig. 4), the same pair of lines can

likewise be observed, although they are less easily recognised due to broadening. The observed splitting might be caused by an exchange interaction of 0.0056 cm^{-1}. The splitting in the $g_{\|}$ part of the spectrum is more complex. The Q-band spectrum (Fig. 2, trace A) shows that four absorption lines, apparently grouped into two pairs, are present. If we assume that the high-field pair of lines at Q- and X-band belong together, then a tentative interpretation of the spectra at the three frequency bands might be as follows. The g_z line in the Q-band spectrum is split up in two times two lines (see the bars under trace A in Fig. 2). In that case, the distance between $g_{\|} = 1.9712$ and the centre of the high-field pair of lines would be 5.8, 4.0 (Fig. 2, trace C) and 2.5 mT (Fig. 4, trace B) at Q-, X- and S-band respectively, whereas the splitting of the pair itself would be 9.1, 3.9 and less than 1.5 mT at the three frequency bands. The splittings are indicated by the horizontal bars in Figs. 2 and 4. We do not understand this behaviour, but we realise that with regard to the theoretical complexity of the system at hand [41], the latter analysis might be a naive one.

Phenomenologically the spectra of signal 4 and signal 2 at the three frequencies resemble the computed spectra of the spin-coupled Co(II)-radical pair given by Buettner and Coffman [42] at similar microwave frequencies. Disregarding the nuclear hyperfine interaction, the Co(II) from Buettner and Coffman can be compared with the Ni(III) in our case. Both are low-spin d^7 ions with very similar g values. The radical from the pair treated by Buettner and Coffman has to be replaced in our case by the much more anisotropic $S = 1/2$ system of the Fe-S cluster. Also, the mutual orientation of the g-tensors and the interaction tensors are probably different and we cannot predict off-hand in what way this would change the spectra. We consider the spin-spin interaction to be mainly of the anisotropic-exchange type, but a contribution from dipole-dipole interaction cannot be ruled out. The observed splittings in the spectra indicate that the exchange energy is in the order of 0.01 cm^{-1}. According to Coffman and Buettner [40], this would mean that the distance between the two spin systems is less than 1.2 nm. The temperature dependence of the signals below 15 K (Fig. 10) is consistent with such a weak exchange.

As a result of the interaction with the Fe-S cluster, the spin-relaxation rate of the Ni(III) ion is greatly enhanced compared to that of the magnetically isolated nickel ions. The coupling can be broken by incubation with excess ascorbate plus 5 μM phenazine methosulphate, whereby the signals 2 and 4 disappear and the signals 1 and 3 increase in intensity [16]. Thus, if the [4Fe-4S] cluster, displaying signal 2, degrades to a [3Fe-xS] cluster, characterised by signal 1, the spin-spin interaction is no longer present and the nickel ion, initially detected as a spin-coupled species in signal 4, then becomes magnetically isolated (signal 3). We conclude that during this transition, the ligand field of the nickel ion is not changed but that the spin-spin interaction collapses as a result of the removal of one of the iron ions from the [4Fe-4S] cluster. Exchange interactions, easpecially if weak, usually arise from superexchange via intervening ligand between the two interacting ions [42,44]. In our case, one particular iron ion of the [4Fe-4S] cluster, the one that is displaced on conversion to a 3Fe-cluster [16,34], and also possibly one of its ligands are considered to be essential for the exchange interaction of the $S = 1/2$ system of the cluster with the nickel ion. It may well be that an intact exchange path is also required for H_2: acceptor oxidoreductase activity.

The coordination of Ni(III) in hydrogenase

From the EPR spectra of Ni(III), as observed in intact and irreversibly inactivated hydrogenase molecules, it can be concluded that the ion is in a low-spin $3d^7$ configuration [33,45] and has a rhombically distorted octahedral ligand field [45]. The fact that the g_x and g_y values are greater than the g_z value means that the unpaired electron is in the d_{z^2} orbital [45].

Ni(III) has been the subject of many studies within the field of coordination chemistry (for recent reviews see Refs. 46 and 47). Where organic tetraaza macrocycles were used as ligands, the EPR spectra invariably show axial symmetry with $g_{\perp} > g_{\|}$ [48]. Also, complexes of Ni(III) and a variety of peptides have been observed [49–52]. Very recently [53], peptides containing a sulphydryl group have also been used to investigate the effect of the extra sulphur on the EPR spectrum. It was found [53] that rhombic-type spectra were only

observed if one of the four equatorial N atoms was replaced by sulphur. Addition of an axial histidyl N atom induced nitrogen hyperfine splitting in the g_z line. By comparing these spectra with those of Ni(III) in hydrogenase, Sugiura et al. [53] proposed that the Ni in hydrogenase has one cysteine sulphur as an equatorial ligand in a tetragonal geometry and that an axial N ligand may be ruled out, since there is no hyperfine structure resolved in the g_z line of this nickel.

We notice two main differences between the physical properties of nickel in hydrogenase and in the model-peptide complexes. The first difference is the line width in the EPR spectra. In the published spectra of Ni(III) peptides [51–53], the linewidth in the $g_{x,y}$ region is much greater than that around g_z. This was ascribed to unresolved hyperfine splitting from the equatorial N ligands [51,53]. The effective line width of the $g_{x,y}$ lines is so great that a nitrogen splitting of 2.0 mT would not have been resolved [51]. The EPR spectrum of Ni(III) in hydrogenase has the same (small) line width in the x, y and z direction. Typically, the width of the g_y lines is 1.0–1.3 mT [6,22] and, when present, a hyperfine splitting of 1.5 mT is clearly resolved [6]. Recently, some remarkable, air-stable square-pyramidal coordinated Ni(III) complexes with the general formula $Ni[C_6H_3(CH_2NMe_2)_2\text{-}O,O']X_2$ (X = Cl, Br, I), were introduced by Grove et al. [54]. In the equatorial plane, Ni is coordinated by C (direct Ni-C σ bond) two N atoms and one halo atom. The other halo atom forms an axial ligand to the nickel. All these compounds show rhombic EPR spectra, e.g., the chloro compound has $g_{x,y,z}$ = 2.336, 2.190 and 2.020, values which are very similar to those of nickel in hydrogenase. Also, the g_x and g_y are narrow lines and the spectrum, therefore, greatly resembles that of hydrogenase. The example demonstrates that equatorial N atoms (and halo atoms) can be present without the excessive broadening of the g_x and g_y lines as occurs in nickel peptides [50–52]. We, therefore, suggest that g-strain [27–29] dominates the width of the $g_{x,y}$ lines in the spectra of nickel peptides. The second major difference between the peptide complexes and hydrogenase is the oxidation-reduction potential of the Ni(III)/Ni(II) couple. In the peptide as well as other nickel complexes, the most stable valency state is Ni(II). The E_0 values (as referred to the standard H_2 electrode) for Ni(III)/Ni(II) are between +800 and +1200 mV [48,50,52]. The midpoint redox potential of nickel in hydrogenase is between −150 mV (pH 7.2) [10] and −220 mV (pH 8.5) [13] (and about −175 mV (pH 7.3) in the *C. vinosum* enzyme; J.W. Van der Zwaan, unpublished results).

The rhombically distorted octahedral ligand field of Ni(III) in hydrogenase can be generated by a square-pyramidal (five ligands) or an octahedral (six ligands) coordination. A trigonal-bipyramidal coordination is less likely, since one then would expect the d_{z^2} orbital to be highest in energy. The rhombicity of the EPR spectrum indicates that the four equatorial ligands cannot all have the same character. It must be stressed here that nothing can be concluded at this stage about the chemical identity of these ligands. The absence of hyperfine splitting in the g_z line makes the presence of an axial N atom unlikely [51,53]. Since it is our working hypothesis that Ni in the enzyme is directly involved in the reaction with hydrogen, we believe that the ion has five ligands provided by the protein in a square-pyramidal coordination. Water might serve as a sixth ligand. The difference between Ni-a and Ni-b, as present in the *C. vinosum* hydrogenase, is probably the result of a difference in the equatorial ligand pattern of the two nickel ions.

Concluding remarks

All nickel-containing 'uptake' hydrogenases but one have been shown to contain one or more EPR-detectable, redox-active Fe-S clusters. The enzyme from *M. thermoautotrophicum* strain Marburg is the exception [5,6]. In this case, there is as yet no indication for an Fe-S cluster and only Ni can be detected in the active enzyme as an independent $S = 1/2$ ion. This indicates that this hydrogenase could be active without the presence of an EPR-detectable, redox-active Fe-S cluster. A further investigation of the properties of this particular enzyme might therefore be worthwhile. We suggest that in the other nickel-containing hydrogenases, coupling between the nickel ion and an Fe-S cluster is quite likely to exist. The EPR signals of the Ni detected thus far in these enzymes [9–15] always account for less than half of

the chemically determined Ni. The signals can still be observed at temperatures above 50 K, like the non-interacting Ni, in our irreversibly inactivated enzyme molecules. As in the case of the *C. vinosum* enzyme treated with 2-mercaptoethanol, it might well be that the coupled pair of Ni and Fe-S is not readily EPR-detectable in these enzymes.

Acknowledgements

We thank Professor E.C. Slater for his stimulating interest during this research and for his criticism on the manuscript. We are indebted to Dr. M. Glasbeek for stimulating discussions on the topic of spin-spin interactions. We thank Drs. D.M. Grove and G. Van Koten for fruitful discussions on the properties of Ni complexes. Dr. R. Boelens is acknowledged for some most useful suggestions. We thank the Netherlands Organization for the Advancement of Pure Research (Z.W.O.) for a grant, supplied via the Netherlands Foundation for Chemical Research (S.O.N.), that, in particular, enabled us to buy the 4 GHz microwave equipment.

References

1 Krasna, A.I. (1979) Enzyme Microb. Techn. 1, 165–172
2 Weaver, P.F., Lien, S. and Siebert, M. (1980) Sol. Energy 24, 3–45
3 Adams, M.W.W., Mortenson, L.E. and Chen, J.-S. (1980) Biochim. Biophys. Acta 594, 105–176
4 Friedrich, B., Heine, E., Finck, A. and Friedrich, C.G. (1981) J. Bacteriol. 145, 1144–1149
5 Graf, E.-G. and Thauer, R.K. (1981) FEBS Lett. 136, 165–169
6 Albracht, S.P.J., Graf, E.-G. and Thauer, R.K. (1982) FEBS Lett. 140, 311–313
7 Friedrich, C.G., Schneider, K. and Friedrich, B. (1982) J. Bacteriol. 152, 42–48
8 Jacobson, F.S., Daniels, L., Fox, J.A., Walsh, C.T. and Orme-Johnson, W.H. (1982) J. Biol. Chem. 257, 3385–3388
9 Kojima, N., Fox, J.A., Hausinger, R.P., Daniels, L., Orme-Johnson, W.H. and Walsh, C.T. (1983) Proc. Natl. Acad. Sci. USA 80, 378–382
10 Cammack, R., Patil, D., Aguirre, R. and Hatchikian, E.C. (1982) FEBS Lett. 142, 289–292
11 LeGall, J., Ljungdahl, P.O., Moura, I., Peck, H.D., Jr., Xavier, A.V., Moura, J.J.G., Teixeira, M., Huynh, B.H. and DerVartanian, D.V. (1982) Biochem. Biophys. Res. Commun. 106, 610–616
12 Moura, J.J.G., Moura, I., Huynh, B.H., Krüger, H.-J., Teixeira, M., DuVarney, R.G., DerVartanian, D.V., Ljungdahl, P., Xavier, A.V., Peck, H.D., Jr. and LeGall, J. (1982) Biochem. Biophys. Res. Commun. 108, 1388–1393
13 Teixeira, M., Moura, I., Xavier, A.V., DerVartanian, D.V., LeGall, J., Peck, H.D., Jr., Huynh, B.H. and Moura, J.J.G. (1983) Eur. J. Biochem. 130, 481–484
14 Krüger, H.-J., Huynh, B.H., Ljungdahl, P.O., Xavier, A.V., DerVartanian, D.V., Moura, I., Peck, H.D., Jr., Teixeira, M., Moura, J.J.G. and LeGall, J. (1982) J. Biol. Chem. 257, 14620–14623
15 Lalla-Maharajh, W.V., Hall, D.O., Cammack, R., Rao, K.K. and LeGall, J. (1983) Biochem. J. 209, 445–454
16 Albracht, S.P.J., Albrecht, K.J., Schmedding, D.J.M. and Slater, E.C. (1982) Biochim. Biophys. Acta 681, 330–334
17 Unden, G., Böcher, R., Knecht, J. and Kröger, A. (1982) FEBS Lett. 145, 230–234
18 Lancaster, J.R., Jr. (1982) Science 216, 1324–1325
19 Gitlitz, P.H. and Krasna, A.I. (1975) Biochemistry 14, 2561–2568
20 Strekas, T., Antanaitis, B.C. and Krasna, A.I. (1980) Biochim. Biophys. Acta 616, 1–9
21 Van Heerikhuizen, H., Albracht, S.P.J., Slater, E.C. and Van Rheenen, P.S. (1981) Biochim. Biophys. Acta 657, 26–39
22 Albracht, S.P.J., Kalkman, M.L. and Slater, E.C. (1983) Biochim. Biophys. Acta 724, 309–316
23 Lundin, A. and Aasa, R. (1972) J. Magn. Reson. 8, 70–73
24 Albracht, S.P.J. (1973) J. Magn. Reson. 13, 299–303
25 Albracht, S.P.J., Dooyewaard, G., Leeuwerik, F.J. and Van Swol, B. (1977) Biochim. Biophys. Acta 459, 300–317
26 Albracht, S.P.J. (1980) Biochim. Biophys. Acta 612, 11–28
27 Fritz, J., Anderson, R., Fee, J., Palmer, G., Sands, R.H., Tsibris, J.C.M., Gunsulus, I.C., Orme-Johnson, W.H. and Beinert, H. (1981) Biochim. Biophys. Acta 253, 110–133
28 Hagen, W.R. (1981) J. Mag. Reson. 44, 447–469
29 Hagen, W.R. and Albracht, S.P.J. (1982) Biochim. Biophys. Acta 702, 61–71
30 Mailer, C. and Taylor, C.P.S. (1973) Biochim. Biophys. Acta 322, 195–202
31 Borcherds, P.H. (1969) Cryogenics 9, 138
32 Abragam, A. and Bleany, B. (1970) Electron Paramagnetic Resonance of Transition Ions, Clarendon Press, Oxford
33 Wertz, J.E. and Bolton, J.R. (1972) Electron Spin Resonance. Elementary Theory and Practical Applications, McGraw-Hill, New York
34 Beinert, H. and Thomson, A.J. (1983) Arch. Biochem. Biophys. 222, 333–361
35 Lowe, D.J., Lynden-Bell, R.M. and Bray, R.C. (1972) Biochem. J. 130, 239–249
36 Mathews, R., Charlton, S., Sands, R.H. and Palmer, G. (1974) J. Biol. Chem. 249, 4326–4328
37 Ruzicka, F.J., Beinert, H., Schepler, K.L., Dunham, W.R. and Sands, R.H. (1975) Proc. Natl. Acad. Sci. USA 72, 2886–2890
38 Schepler, K.L., Dunham, W.R., Sands, R.H., Fee, J.A. and Abeles, R.H. (1975) Biochim. Biophys. Acta 397, 510–518
39 Aasa, R., Bergström, J. and Vänngård, T. (1981) Biochim. Biophys. Acta 637, 118–123
40 Coffman, R.E. and Buettner, G.R. (1979) J. Phys. Chem. 83, 2387–2392

41 Coffman, R.E. and Buettner, G.R. (1979) J. Phys. Chem. 83, 2392–2400
42 Buettner, G.R. and Coffman, R.E. (1977) Biochim. Biophys. Acta 480, 495–505
43 Lowe, D.J. and Bray, R.C. (1978) Biochem. J. 169, 471–479
44 Owen, J. and Harris, E.A. (1972) in Electron Paramagnetic Resonance (Geschwind, S., ed.), pp. 427–492, Plenum Press, New York
45 Maki, A.H., Edelstein, N., Davison, A. and Holm, R.H. (1964) J. Am. Chem. Soc. 86, 4580–4587
46 Nag, K. and Chakravortry, A. (1980) Coord. Chem. Rev. 33, 87–147
47 Haines, R.I. and McAnley, A. (1981) Coord. Chem. Rev. 39, 77–119
48 Lovecchio, F.V., Gore, E.S. and Busch, D.H. (1974) J. Am. Chem. Soc. 96, 3109–3118
49 Freeman, H.C., Guss, J.M. and Sinclair, R.L. (1968) J. Chem. Soc. Chem. Commun. 485–487
50 Bossu, F.P. and Margerum, D.W. (1977) Inorg. Chem. 16, 1210–1214
51 Lappin, A.G., Murray, C.K. and Margerum, D.W. (1978) Inorg. Chem. 17, 1630–1634
52 Sakurai, T., Hongo, J.-I., Nakahara, A. and Nakao, Y. (1980) Inorg. Chim. Acta 46, 205–210
53 Sugiura, Y., Kuwahara, J. and Suzuki, T. (1983) Biochem. Biophys. Res. Commun. 115, 878–881
54 Grove, D.M., Van Koten, G., Zoet, R., Murrall, N.W. and Welch, A.J. (1983) J. Am. Chem. Soc. 105, 1379–1380